JOURNAL OF CATALYSIS **171,** 476–484 (1997)
ARTICLE NO. CA971827

Decomposition and Oxidation of Dimethyl Ether on Rh Catalysts

F. Solymosi, J. Cserényi, and L. Ovári

Institute of Solid State and Radiochemistry, A. József University and Reaction Kinetics Research Group of the Hungarian Academy of Sciences,[1] *P.O. Box 168, H-6701, Szeged, Hungary*

Received March 17, 1997; revised July 1, 1997; accepted July 11, 1997

The adsorption, decomposition, and oxidation of dimethyl ether have been investigated on Rh catalyst using alumina, magnesia, titania, and silica supports. Transmission infrared spectroscopic measurements have revealed that adsorbed ether molecules are transformed into methoxy species at 200–300 K. This process proceeds mainly on the supports. The effect of Rh is exhibited at higher temperature, above 473 K, when it catalyses the decomposition of dimethyl ether to give CO, H_2, and a small amount of CH_4. The formation of strongly adsorbed species, such as CO, CH_x, and C, leads to the early deactivation of the catalysts. The complete oxidation of dimethyl ether to CO_2 and H_2O was studied in a flow system. The reaction started above 450 K and attained almost 100% conversion at 600–630 K for all supported Rh, except Rh/MgO. There are no significant differences in the activities of other Rh samples. Taking into account the dispersities of Rh, the most effective catalyst is the alumina-, followed by titania-, silica-, and magnesia-supported Rh. Whereas at lower temperatures different hydrocarbons in minor amounts were detected in the products, above 600 K only 0.1–0.2% methane was identified. Based on the results obtained on Rh(111) under UHV conditions, it is concluded that dimethyl ether interacts with adsorbed O atoms bonded to the Rh, and the oxidation proceeds via the transient formation of methoxy species on the Rh.

1. INTRODUCTION

The study of the adsorption and catalytic reaction of dimethyl ether (DME) is motivated by several reasons. DME is a key compound in the conversion of methanol to gasoline (1, 2), which is one of the most successful industrial catalytic processes. Recently, it has been proposed to use DME as an alternative fuel for diesel engines (3, 4). It is claimed that the burning of DME produces much less pollutants compared to diesel oil and satisfies worldwide emission standards (1–3) .

In our laboratory we are mainly concerned with the interaction of DME with catalyst surface and with its complete oxidation, assuming that exhaust catalysts may remain in use even after the application of DME as a fuel. In a recent comparative work we found that alumina-supported platinum metals catalyse the total oxidation of DME above 473 K, and 100% conversion can be attained at 673–723 K (5). As regards the decomposition of DME, Rh/Al_2O_3 was one of the most active catalysts, it deactivated, however, very easily. The interaction of DME with clean and K-promoted Rh(111) has been also examined by high resolution electron energy loss spectroscopy (HREELS) and the primary dissociation products have been established (6, 7).

In the present paper we performed detailed studies on supported Rh catalysts. Attention is paid to the adsorption, decomposition, and oxidation of DME. The effects of support materials are also explored for all these processes.

2. EXPERIMENTAL

The oxide supports were impregnated at room temperature in an aqueous solution of $RhCl_3 \cdot 3H_2O$ (Johnson–Matthey). The amount of $RhCl_3 \cdot 3H_2O$ used was calculated so, that if it will be transformed into metallic Rh (following oxidation and reduction), it should correspond to 1 wt% of the catalyst. The impregnated material was dried at 330 K and stored over silica gel. The following supports were used: Al_2O_3 (Degussa P 110 C1), TiO_2 (Degussa P 25), SiO_2 (Cab-O-Sil) and MgO (DAB 6). The fragments of catalyst pellets were oxidized at 673 K for 30 min and reduced at 773 K in the catalytic reactor for 1 h. In the case of Rh/TiO_2 the effects of low and high temperature reduction were also examined. When the effects of oxidized Rh/Al_2O_2 was tested the reduction step was omitted. XPS analysis showed that in the oxidized sample, ~70% of the Rh was in the state of Rh^{3+}. DME was the product of Aldrich. The gases used were initially of commercial purity. The Ar (99.995) was deoxygenated with an oxytrap. The other impurities were adsorbed by a 5A molecular sieve at the temperature of liquid nitrogen.

Catalytic measurements were carried out in a fixed bed continuous-flow reactor made of quartz (17 mm ID). The amount of catalysts used was 0.3 g. Analyses of the exit

[1] This laboratory is a part of the Center for Catalysis, Surface and Material Science at the University of Szeged.

0021-9517/97 $25.00

TABLE 1

Some Characteristic Data for Supported Rh

Supports	Surface area of the support (m^2/g)	Dispersion of Rh (%)	Mean particle diameter of Rh (Å)	TOF[b] (s^{-1})
Al_2O_3 (Degussa P 110 C1)	100	38.3	22.6	0.022
TiO_2 (Degussa P 25)	150	4.4	—	—
		30.4[a]	28.4	0.021
SiO_2 (Cab-O-Sil)	200	45.5	19.0	0.019
MgO DAB C	170	4.8	—	(0.003)

[a] In this case the reduction temperature was 673 K.

[b] Turnover frequency for the oxidation of DME on supported Rh catalysts under isotherm conditions at 523 K. Rates of CO_2 formation were related to the number of surface Rh atoms.

gases were performed with a Hewlett–Packard 5890 gas chromatograph using Porapak QS column. The absence of diffusion limitation was confirmed by the method of Kőrös and Novak (8). The system was operated at a total pressure of 1 atm. The carrier gas was argon. In the study of the decomposition of DME it contained 10.0 vol% DME. In the oxidation of DME, the carrier gas contained 1 vol% DME and 5 vol% O_2. In both cases the flow rate was 20 ml/min. Note that the experimental conditions were outside of both the lower (2 vol%) and the higher (27 vol%) explosion limit of DME in air.

Infrared spectroscopic studies were made in a vacuum IR cell using self-supporting wafers of catalyst powders (30×30 mm, ≈ 20 mg/cm^2) which underwent the same pretreatments as before catalytic measurements. The IR cell used made it possible to register the spectra between 100–300 K. Spectra were recorded with a Biorad (Digilab. Div.) Fourier transform IR spectrometer (FTS 155).

The dispersity of the supported metals was determined by hydrogen adsorption at 300 K. Data are listed in Table 1.

3. RESULTS

3.1. Interaction of DME with Rh Catalysts

The interaction of DME with Rh catalysts was first investigated by means of infrared (IR) spectroscopy. In order to minimize the thermal dissociation, DME was adsorbed on the catalyst samples at 110–130 K. Afterwards the IR cell was evacuated and the catalysts were warmed under continuous pumping conditions to higher temperatures. In the presence of DME vapor we identified the characteristic absorption bands of gaseous DME (Table 2). These bands were detected at somewhat different positions for all samples following the evacuation at 120–140 K.

During annealing the adsorbed layer over Rh/Al_2O_3, the first spectral changes, indicating the formation of new surface species, occurred at 200 K (Fig. 1A). The positions of absorption bands were 2960, 2879, 2841, 1472, 1461, 1259, 1157, and 1061 cm^{-1}. Further annealing the sample up to 300 K, a slight attenuation of these bands was observed. These bands differ from those due to adsorbed DME and agree well with the absorption bands attributed to the vibration of methoxy species (Table 2).

Similar features were experienced for Rh/TiO_2 and Rh/MgO with the difference that the new absorption bands produced were weaker and appeared at somewhat lower frequencies compared to Rh/Al_2O_3. This was more expressed for Rh/MgO (Figs. 1B and C). The absorption bands of DME were also identified for Rh/SiO_2 at 130–150 K, which attenuated and finally disappeared after gradually heating the adsorbed layer to 300 K without any change in their positions.

When the adsorption of DME was performed at 300 K, we detected the same absorption bands as were observed previously after heating the adsorbed layer from 150 to 250–300 K (Fig. 1). In addition, we found a weak band in the region of CO stretching frequency at 2020–2042 cm^{-1}. Following heating the adsorbed layer under continuous evacuation led to a decay in the intensities of all the bands with the exception of the CO band. The latter grew and attained the highest intensity at 450–500 K, where all the other bands disappeared or became extremely weak (Fig. 2). These features very likely correspond to the complete decomposition of methoxy species located on supports. Adsorption of DME on Rh/SiO_2 at 300 K produced weak bands corresponding to adsorbed DME. After the adsorbed layer is heated to 300–400 K, two very weak spectral features remained at 2859 and 2947 cm^{-1}, and a CO band also developed (Fig. 3).

TABLE 2

Vibrational Frequencies (cm^{-1}) of Gaseous and Adsorbed DME on Rh-free Supports

Mode	$(CH_3)_2O_{(g)}$[a]	$(CH_3)_2O/Al_2O_3$[b]	Al_2O_3[c]	TiO_2[c]	MgO[c]
$\nu_{as}(CH_3)$	2996*	2984	2962	2952	2938
	2925	2922			
$2\delta(CH_3)$	2887	2890	—	—	—
		2872			
$\nu_s(CH_3)$	2817	2821	2845	2839	2821
$\delta(CH_3)$	1470	1477	1473	1470	1465
	1456	1459	1458		
$\gamma(CH_3)$	1244	(1252)	(1261)	(1250)	1155
	1179	1166	1157	1156	
$\nu_{as}(CO)$	1102	1092	1060	1068	1058

[a] Gaseous DME (Ref. (10)).

[b] Adsorbed DME on Al_2O_3 at 150 K (Ref. (10)).

[c] After heating the adsorbed DME on Rh-free supports to 290 K (Ref. (16)).

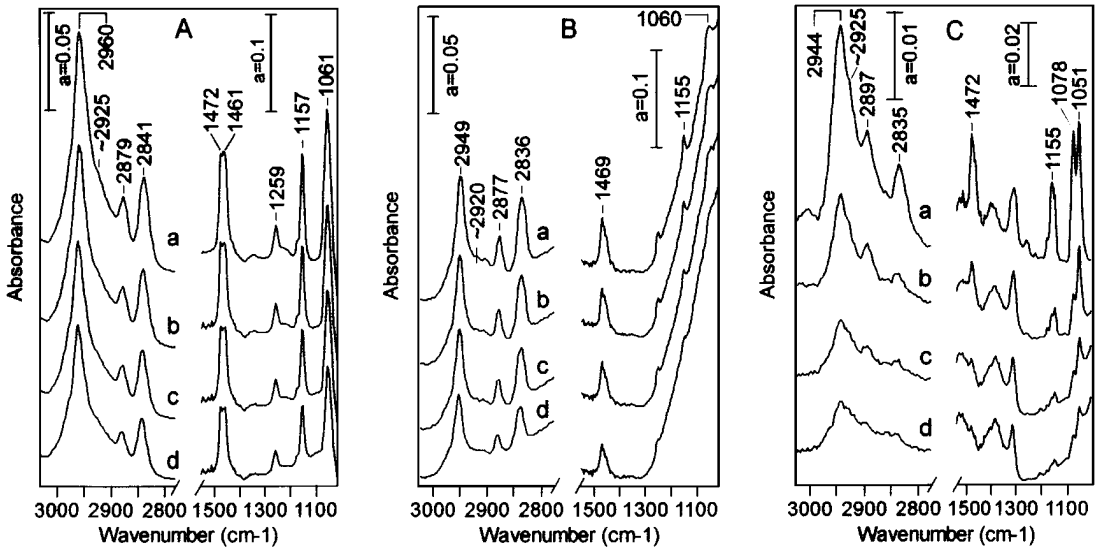

FIG. 1. Infrared spectra of DME adsorbed on supported Rh catalysts recorded as a function of temperature during continuous evacuation. DME was adsorbed at 130 K: (A) Rh/Al_2O_3; (B) Rh/TiO_2; (C) Rh/MgO. (a) 200 K, (b) 220 K, (c) 250 K, and (d) 300 K.

3.2. Thermal Decomposition of DME

Measurable decomposition of DME was observed at 523 K. Results for the four catalyst samples are presented in Fig. 4A. The highest initial conversion (25%) was exhibited by Rh/Al_2O_3, which decayed abruptly to 5%, and gradually to about 0.5%. The main products of the decomposition were H_2, CO, and CH_4. The selectivity to CO varied between 34–55% and that to CH_4 between 15–51%. In very small amounts, methanol, ethane, and propane were also detected (Fig. 4B). The high initial activity can be restored by the oxidation and reduction of the catalyst. Although Rh/TiO_2 and Rh/SiO_2 were less active catalysts, a decay in the conversion of DME was also observed. A very low activity was found for Rh/MgO. Note that a decrease in the reduction temperature of Rh/TiO_2 from 773 to 673 K enhanced its catalytic activity by a factor of 6.

The catalytic influence of the support materials has been also tested under the same conditions. The highest initial activity (0.18% DME conversion) was measured for alumina. The other supports exhibited even less activity if at all.

In order to establish the possible reasons of the deactivation of the Rh/Al_2O_3 several measurements have been performed. First we determined the uptake of CO on fresh and used catalysts. We found that after DME treatment for

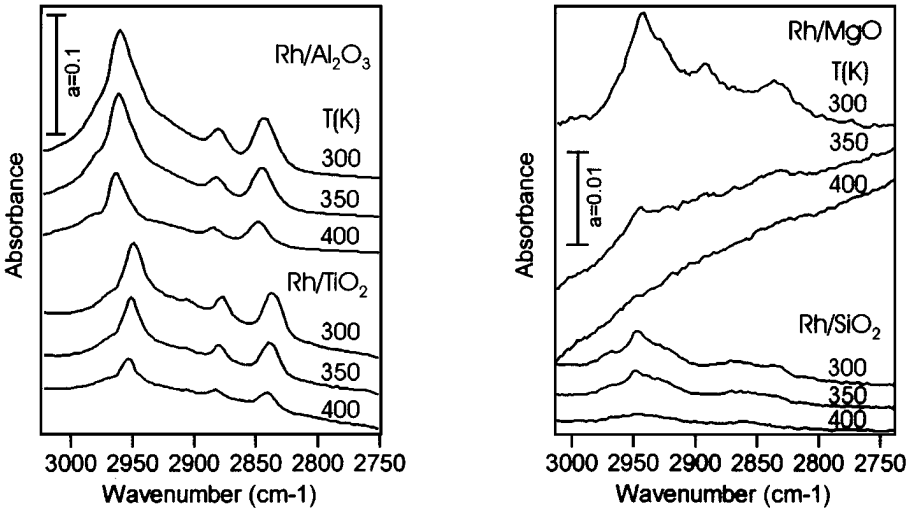

FIG. 2. Infrared spectra of DME adsorbed on supported Rh catalysts recorded as a function of temperature during continuous evacuation. DME was adsorbed at 300 K.

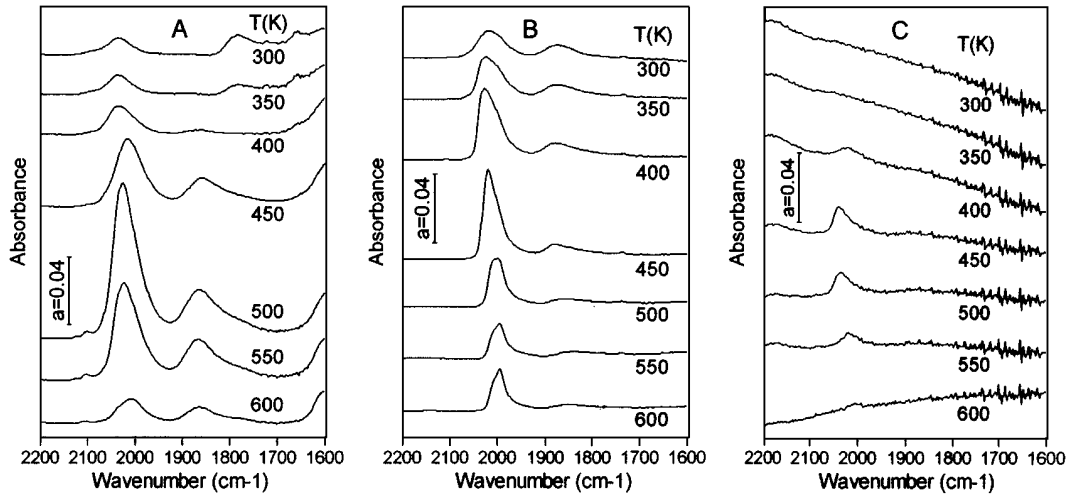

FIG. 3. Formation of the CO bands following the annealing of adsorbed DME on Rh catalysts: (A) Rh/Al_2O_3; (B) Rh/TiO_2; (C) Rh/SiO_2.

90 min the uptake of CO at 300 K decreased by 60–70%. In harmony with this, while the adsorption of CO on an untreated catalyst gave intense absorption bands at 2107 and 2040 cm^{-1} and a less intense one at 2078 cm^{-1}, after DME treatment at 523 K for 90 min, the CO bands shifted to lower frequencies and were of much less intensities. It is important to note that there were no significant spectral changes in the presence of CO even after extended adsorption time (Fig. 5).

We also performed TPD and TPR measurements after 2 h of reaction on Rh/Al_2O_3. In the TPD we found the desorption of CH_4 ($T_p = 637$ K), CO ($T_p = 605$ K), and H_2 ($T_p = 605$ K). The desorption of H_2O was also observed during the heating up of the sample, but no peak could be resolved. Some TPD curves are presented in Fig. 6A. After desorbing these products, TPR measurements were carried out in the presence of H_2 flow. The evolution of methane started at 390 K and did not cease up to 900 K. Two sharper peaks appeared at 445 and 780 K. The amount of $C + CH_x$ was also determined by temperature-programmed oxidation (TPO). Independently of the nature of the support, the oxidation started at lower temperatures, above 330 K, reached the highest rate at 450 K and yielded only CO_2 and H_2O.

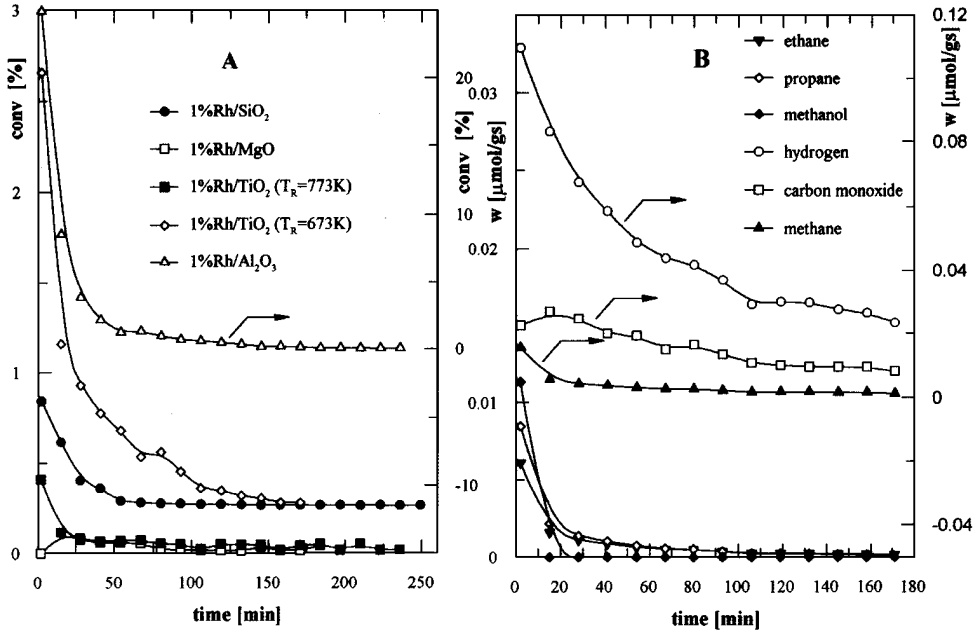

FIG. 4. (A) Thermal decomposition of DME on supported Rh catalysts at 523 K in a flow system. (B) The products of the decomposition of DME on Rh/Al_2O_3 at 523 K.

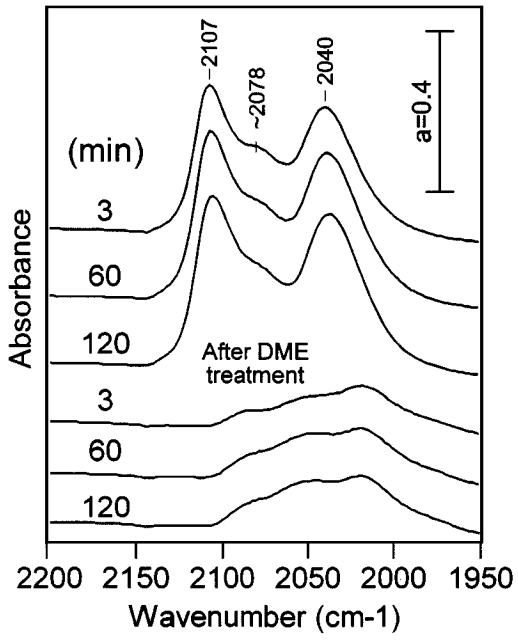

FIG. 5. FTIR spectra following CO adsorption at 300 K on unused Rh/Al_2O_3 and with DME-treated Rh/Al_2O_3 samples at 523 K.

3.3. Oxidation of DME

In the first series of measurements the oxidation of DME was studied by gradually heating the catalyst bed in the presence of reacting gas mixture from 300 K. The conversion-temperature curves are shown in Fig. 7A. The reaction began slightly above 450 K. A complete oxidation was achieved at the lowest temperature for Rh/SiO_2 followed by Rh/TiO_2 and Rh/Al_2O_3. The catalytic performance of Rh/TiO_2 was somewhat higher when it was reduced at 673 K. Less active catalyst was again the Rh/MgO, where the conversion of DME was only 36–38% at 673 K and 100% of conversion was attained only at 873 K.

According to the analysis, the total oxidation of DME can be described by the equation

$$CH_3{-}O{-}CH_3 + 3O_2 = 2CO_2 + 3H_2O. \qquad [1]$$

At lower temperatures, below 573–600 K, small amounts of CH_4, C_2H_6, C_3H_8, and CH_3OH were also produced. Above ~600 K, however, only CH_4 was detected in traces. At the conversion of 90–95%, the selectivity to CO_2 formation (based on C-containing gaseous compounds) is around 96–98% on all catalyst samples. Note that the atomic balances on C and H_2 correspond well to the calculated values (95 and 97%).

The oxidation of DME also occurred on pure supports but at significantly higher temperatures (Fig. 7B). The most active support was titania followed by alumina, silica, and magnesia. In the empty reactor the reaction began only above 873 K.

The oxidation of DME was also studied under isotherm conditions in time on stream at 523 K. Data are presented in Fig. 8A. Almost 65–70% conversion of DME was measured for Rh/Al_2O_3 and Rh/SiO_2. No decay in the performance of the catalyst occurred in 4 h. High rate of oxidation was measured for Rh/TiO_2 samples. Only a very slight oxidation of DME was observed at this temperature on Rh/MgO. Apart

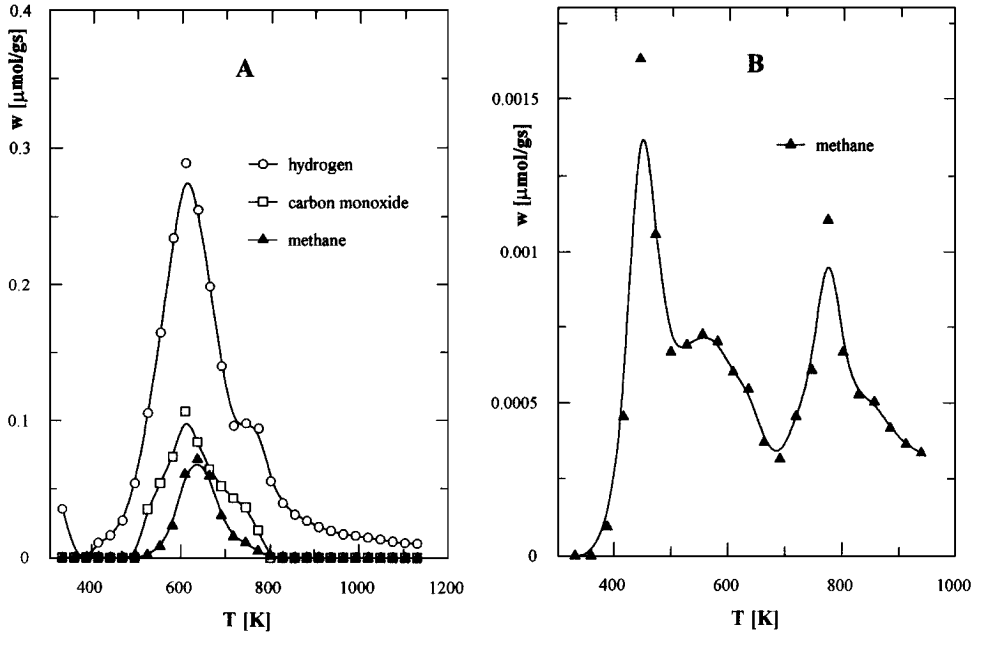

FIG. 6. (A) Temperature programmed desorption (TPD) following the decomposition of DME on Rh/Al_2O_3 at 523 K for 2 h. (B) After TPD, the sample was cooled in He to room temperature, heated up in the H_2 flow (TPR experiment), and the amount of methane produced was determined.

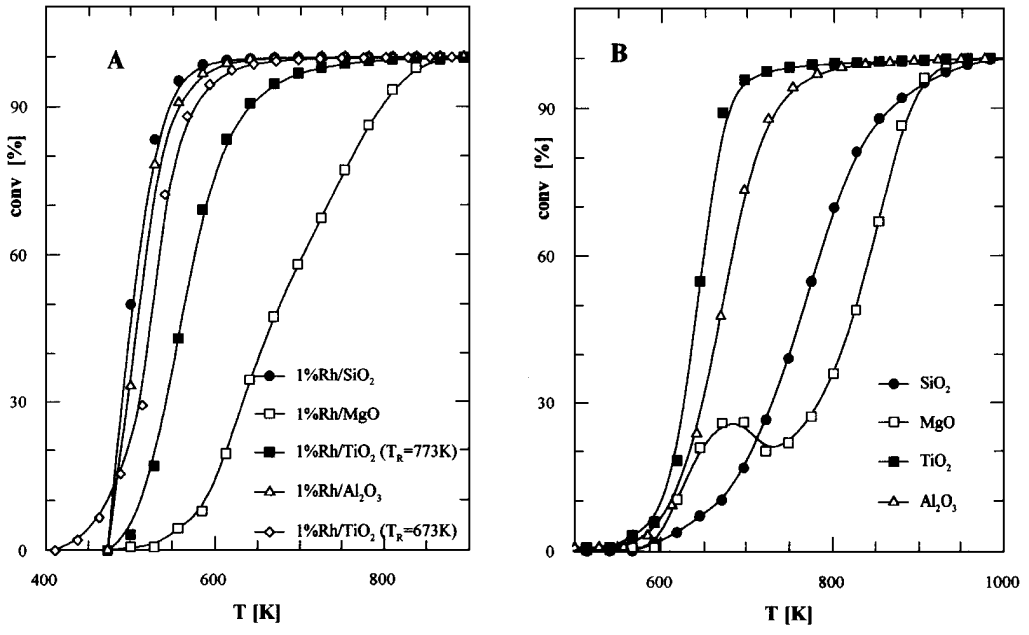

FIG. 7. (A) Oxidation of DME on supported Rh catalysts and (B) on Rh-free supports at different temperatures in a flow system as a function of temperature.

from the very low activity of Rh/MgO, no support effect was observed: the turnover frequencies were practically the same for the three active catalysts (Table 1).

From the variation of the space velocity for Rh/Al_2O_3 we obtained that the rate of the oxidation of DME increased linearly with the increase of the space velocity (Fig. 8B). On this catalyst we determined the effect of the partial pressure of reactants on the rate of oxidation of DME. We found that an increase in the concentration of both compounds increased the rate of oxidation. The kinetic order with respect to O_2 was found to be 0.4. The order with respect to DME is about 0.8.

In order to know more about the interaction of DME with the catalyst, the reaction of DME with reduced and oxidized

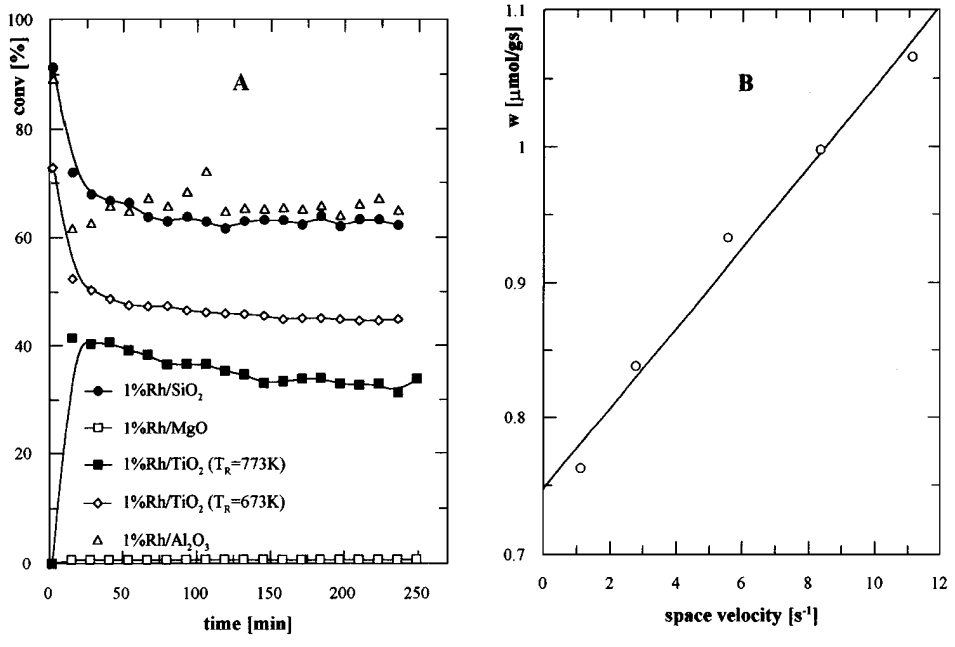

FIG. 8. (A) Oxidation of DME on supported Rh catalysts under isotherm conditions at 523 K. (B) Dependence of the rate of CO_2 formation on the space velocity in the oxidation of DME on Rh/Al_2O_3 at 523 K.

Rh/Al_2O_3 was also followed by pulse technique at 523 K. One pulse contained 1.56 μmol of DME. Assuming that the oxidized Rh is in the form of Rh_2O_3, the complete oxidation of one pulse of DME requires 24% of the oxygen of Rh_2O_3. In the case of reduced sample CO, H_2, and CH_4 were the main products with minor amounts of ethane, methanol, and propane. The rates of their formation were practically constant during the use of 40 DME pulses. On the oxidized sample the primary products were CO_2 and H_2O. With the progress of the reduction of rhodium oxide, the amount of these compounds gradually decreased and the formation of CO, CH_4, C_2H_6 and somewhat later methanol came into prominence. The formation of the latter compound showed a maximum when the production of CO_2 and H_2O ceased.

4. DISCUSSION

4.1. Interaction of DME with Solid Surfaces

There is very little information concerning the interaction of DME with oxides. The adsorption of DME on alumina has been studied by Yakerson *et al.* (9) and Yates *et al.* (10) by means of IR spectroscopy. It was found that DME molecularly adsorbs on alumina, via hydrogen bonding to the surface hydroxyl groups, at 150 K. Heating the adsorbed layer to >250 K caused the desorption of the ether and the formation of surface methoxy species (10). Recently, the adsorption of DME on the protonated ZSM-5 zeolite was investigated by FTIR spectroscopy (11). Results indicated that DME molecules adsorbed on the OH groups by hydrogen bonding irrespective of the acidity of the OH groups and that the oxonium ions of DME were not produced on the studied surface.

DME is rather unreactive on metal surfaces. At low temperature, at 100 K, it adsorbs molecularly on Pt(111), Cu(100), and Al(111) surfaces and desorbs without undergoing dissociation (13, 14). On polycrystalline Pd, DME underwent a thermally activated decomposition at 300 K yielding CO and H (15). Recently the interaction of DME with Rh(111) was studied in our laboratory by HREELS (7). Following the low temperature adsorption, only molecular adsorption and desorption were experienced. The situation was different when the adsorption temperature was raised to 250–300 K. In this case CHO and/or CH_xOCH_x were identified, which decomposed to CO and H_2 at higher temperatures. Vibration losses of adsorbed DME, CH_3, and CH_3O were not seen in the HREEL spectra. On O-dosed Rh(111), however, methoxy species was identified. The presence of K adatoms promoted the dissociation of DME and stabilized the primary products of its dissociation (8).

4.2. Adsorption and Decomposition of DME on Supported Rh

For the interpretation of the IR spectroscopic results obtained on supported Rh, the IR characteristics of DME adsorbed on oxidic supports under the same conditions are of great use (16). The important absorption bands and their assignements are listed in Table 2. The main feature of the adsorbed DME on oxides is its partial transformation into methoxy species around 200 K. This process was first established on alumina surface by Yates *et al.* (10). The disappearance of absorption bands at 2922, 2821, and 1092 cm^{-1} and the appearance of bands at 2962, 2848, and 1059 cm^{-1} were considered as evidence for the transformation of adsorbed DME into methoxy species (10). Following the adsorption of DME on oxides at and above 300 K, this transformation occurred instantaneously. Silica represents a special case as it exhibits a rather low tendency toward methoxy formation. The weak absorption bands at 2859 and 2947 cm^{-1} observed after annealing the adsorbed DME to 350–400 K agree well with the bands at 2860 and 2956 cm^{-1} obtained following the esterification of SiOH with CH_3OH (17, 18). These bands were attributed to the formation of $Si{-}O{-}CH_3$ surface complex (17). Note that the formation of $Si{-}O{-}CH_3$ was recently observed in the interaction of CH_3OH and CH_3Cl with silica and with silica supported metals (19–21).

In the presence of 1% Rh we found the same spectral features as determined for Rh-free supports at 110–290 K (Fig. 1). Accordingly, the adsorption and the transformation of DME into methoxy is practically unaltered by Rh in this temperature range. This is not surprising taking into account the high surface area of the supports. Performing the adsorption on supported Rh at 300 K, and annealing the adsorbed layer under continuous evacuation, we observed that, in addition to the absorption bands of methoxy, a CO band developed at 2020–2041 cm^{-1} for all Rh samples (Fig. 3). Its intensity increased up to 450–500 K with the concomitant attenuation of the methoxy bands (Fig. 2). These features suggest that the methoxy species, located on the oxides, migrated to the Rh_x, where it underwent decomposition

$$CH_3O_{(a)} = CO_{(a)} + 3H_{(a)}. \quad [1]$$

We cannot exclude that a small fraction of methoxy species may exist on Rh_x itself. Following the adsorption of CH_3OH on Rh(111) surface, it was found that the stability region of methoxy on Rh(111) is very narrow; it decomposes readily below 300 K (22, 23).

In many respects similar processes proceeded during the high temperature decomposition of DME under dynamic conditions. The decomposition products identified by gas chromatograph are H_2, CO, and CH_4 with minor amounts of methanol, ethane and propane. The decomposition follows first-order kinetics. In the decomposition we may count with the following steps

$$CH_3OCH_{3(g)} = CH_3OCH_{3(a)} \quad [2]$$

$$CH_3OCH_{3(a)} = CH_{3(a)} + CH_3O_{(a)} \quad [3]$$

$$CH_3O_{(a)} = CO + 1.5\,H_2 \quad [4]$$

$$2CH_{3(a)} = C_2H_{6(g)} \quad [5]$$

$$CH_{3(a)} = C + 1.5\,H_{2(g)} \quad [6]$$

$$CH_{3(a)} + H_{(a)} = CH_{4(g)}. \quad [7]$$

The coupling of CH_3 to C_2H_6 is very limited as only a very small amount of ethane was identified in the products. It is very likely that the decomposition of CH_3 to carbon proceeds through the transient formation of CH_2 and CH species. The formation of a small amount of propane is probably the result of the combination of C_2H_6 with CH_2.

An alternative route of the decomposition of DME is its partial dehydrogenation via the transient formation of $[CH_x{-}O{-}CH_x]$ adsorbed complex which would decompose through CH and CHO species to H, C, and CO. In the study of the interaction of DME with a clean Rh(111) at and above 250 K, where DME is not stable on the surface, we detected CO and H_2 without any CH_4 (7). By means of HREELS we identified a vibration loss at 1235 cm^{-1} which we attributed to the C–O stretching mode [ν(CO)] of η^2-HCO. On the basis of these findings it was concluded that the major pathway of the decomposition of DME on Rh(111) is its partial dehydrogenation. The primary dissociation to adsorbed CH_3 and CH_3O represents only a minor, undetectable step.

In the present case, however, working at higher pressure and using oxidic supports the reaction (3) is the primary process as the adsorption of DME on the supports gives methoxy complex and we measured significant amount of methane among the products.

The interesting feature of the decomposition of DME on Rh/Al_2O_3 is the dramatic decay in the catalytic effect at the very beginning of the reaction. The possible reasons are (i) blocking the active area of Rh by strongly adsorbed species, (ii) a decrease in the dispersion of Rh due to agglomerization of Rh, (iii) deactivation of the metal/support interface particularly effective for the activation of DME. Let us examine these possibilities separately. From the study of the uptake of CO we measured by about 60–70% less CO adsorption on used catalyst compared to the unused sample. This is consistent with the IR spectrum of used sample which showed that a significant amount of CO remained on the surface after DME decomposition. In addition, whereas the adsorption of CO produces an intense pair of the dicarbonyl ($Rh^1(CO)_2$) species on a fresh catalyst, on used catalyst the development of the dicarbonyl species is very limited. This is a strong indication of the agglomeration and deactivation of Rh particles (24, 25). It has been established before that the formation of $Rh^1(CO)_2$ species from Rh_x cluster is the result of the CO-induced disruption of Rh_x crystallites (24–29). The combined TPD and TPR measurements revealed that in addition to adsorbed CO other species are also present on the catalyst (Fig. 6). The evolution of a large amount of hydrogen deserves special attention. Its peak temperature is 590–600 K, which is much higher than that measured following the adsorption of hydrogen on the same surface. This suggests that the hydrogen evolution from the used catalyst may stem from the decomposition of strongly adsorbed hydrocarbon species, which is also responsible for the release of methane at this temperature.

4.4. *Oxidation of DME*

An interesting feature of the complete oxidation of DME over supported Rh is the lack of the deactivation of the catalysts which is in contrast with the catalytic decomposition of DME. This suggests that the strongly adsorbed species formed in the decomposition on Rh are not produced in the oxidation reaction nor are they also oxidized. Another behavior worth mentioning is that the specific activity of Rh is practically the same for all samples, except that for the Rh/MgO (Table 1).

In the oxidation of DME we may consider two major routes. (i) The activation of DME, which consists of the following steps: formation of methoxy species on the supports, migration of this species to the Rh, decomposition of CH_3O at the metal/support interface, and the oxidation of its decomposition products. (ii) Another possibility is the activation of DME by the adsorbed oxygen atoms bonded to the Rh to give a transient surface compound

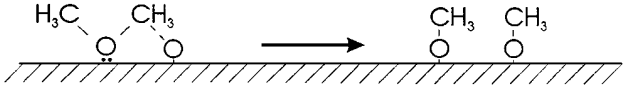

the decomposition of which results in the formation of adsorbed CH_3O on the Rh itself. This reaction channel is supported by the results obtained on Rh(111) under UHV conditions (7). Following the adsorption of DME on O-covered Rh(111), we observed the characteristic vibrations of CH_3O complex. This surface compound may react with other adsorbed O atoms to give CO_2 and H_2O, or it decomposes to adsorbed CO and H, which are subsequently oxidized. The fact that *in situ* FTIR spectra always showed the presence of adsorbed CO even during the high temperature oxidation suggests the importance of the second possibility.

As regards the importance of the two main routes it should be kept in mind that the adsorption and dissociation of DME on silica is very limited compared to other supports (16). At the same time, the catalytic efficiency of Rh/SiO_2 is almost the same as that of Rh/Al_2O_3 (Figs. 7, 8 and Table 1). This feature suggests that the reactions occurring on the supports (formation and migration of methoxy) do not play an important role in the complete oxidation of DME on supported Rh catalysts.

CONCLUSIONS

(i) Dimethyl ether adsorbed on supported Rh is transformed into methoxy species at 200–300 K. The reaction occurs on the supports and is influenced only slightly with the presence of Rh.

(ii) The decomposition of ether molecules is catalysed by Rh above 473 K to give CO, H_2, and small amounts of hydrocarbon products. Rhodium loses its catalytic activity due to the strongly adsorbed species formed in the decomposition.

(iii) In contrast, supported Rh samples exhibited high and constant activity in the total oxidation of dimethyl ether; 100% conversion was reached at 600–650 K.

(iv) It is assumed that the oxidation reaction proceeds through the activation of dimethyl ether by adsorbed O atoms and the transient formation of methoxy species on Rh.

ACKNOWLEDGMENTS

Financial support of this work by OTKA (contract No. T 022869) and loan of rhodium chloride from Johnson–Matthey are greatfully acknowledged.

REFERENCES

1. Meisel, S. L., McCullogh, J. P., Lechthaler, C. H., and Weisz, P. B., *CHEMTECH* **6**, 86 (1976). [Chang, C. D., "Hydrocarbons from Methanol," Dekker, New York, 1983]
2. Spivey, J. J., *Chem. Eng. Commun.* **110**, 123 (1991).
3. Rouhi, A. M., *C&EN* **May 29**, 37 (1995).
4. Fleish, T., Basu, A., Gradassi, M. J., and Masin, J. G., *Stud. Surf. Sci. Catal.* **107**, 117 (1997).
5. Solymosi, F., Cserényi, J., and Ovári, L., *Catal. Lett.* **44**, 89 (1997).
6. Bugyi, L., and Solymosi, F., *Surf. Sci.*, in press.
7. Klivényi, G., and Solymosi, F., to be published.
8. Kőrös, R. M., and Novák, J. M., *J. Chem. Eng. Sci.* **22**, 470 (1967).
9. Yakerson, V. I., Lafer, L. N., Danyushevski, V. Ya., and Rubinshtein, A. M., *Akad Nauk SSSR Ser. Khim.* **11**, 2246 (1967).
10. Chen, J. G., Basu, P., Ballinger, T. H., and Yates, J. T., *Langmuir* **5**, 352 (1989).
11. Fujino, T., Kashitani, M., Kondo, J. N., Domen, K., Hirose, C., Ishida, M., Goto, F., and Wakabayashi, F., *J. Phys. Chem.* **100**, 11649 (1996).
12. Kanazawa, Y., and Nukada, K., *Bull. Chem. Soc. Jpn.* **35**, 612 (1962). [Kiselev, A. V., and Lygin, V. I., "Infrared Spectra of Surface Compounds," Wiley, New York, 1975]
13. Sexton, B. A., and Hughes, A. E., *Surf. Sci.* **140**, 227 (1984).
14. Ng, L., Chen, J. G., Basu, P., and Yates, J. T., Jr., *Langmuir* **3**, 1161 (1987).
15. Lüth, H., Rubloff, G. W., and Grobman, W. B., *Surf. Sci.* **63**, 325 (1977).
16. Ovári, L., and Solymosi, F., to be published.
17. Borello, E., Zecchina, A., and Morterra, C., *J. Phys. Chem.* **71**, 2938, 2945 (1967).
18. Kitahara, S., *Bull. Chem. Soc. Jpn.* **49**, 3389 (1976). [Takezawa, N., and Kobayashi, H., *J. Catal.* **25,** 179 (1972)]
19. Raskó, J., Bontovics, J., and Solymosi, F., *J. Catal.* **143**, 138 (1993).
20. Raskó, J., Bontovics, J., and Solymosi, F., *J. Catal.* **146**, 22 (1994).
21. Driessen, M. D., and Grassian, V. H., *J. Catal.* **161**, 810 (1996).
22. Solymosi, F., Berkó, A., and Tarnóczi, T. I., *Surf. Sci.* **141**, 533 (1984). [Solymosi, F., Berkó, A., and Tarnóczi, T. I., *J. Phys. Chem.* **88,** 6170 (1984)]
23. Houtman, C., and Barteau, M. A., *Surf. Sci.* **248**, 57 (1991). [Houtman, C., and Barteau, M. A., *Langmuir* **6,** 1558 (1990)]
24. Solymosi, F., and Pásztor, M., *J. Phys. Chem.* **89**, 4789 (1985). [Solymosi, F., and Pásztor, M., *J. Phys. Chem.* **90**, 5312 (1986)]
25. Solymosi, F., and Bánsági, T., *J. Phys. Chem.* **97**, 10133 (1993).
26. Van't Bilk, H. F. J., Van Zon, J. B. A. D., Huizinga, T., Vis, J. C., Koningsberger, D. C., and Prins, R., *J. Amer. Chem. Soc.* **107**, 3139 (1985).
27. Zaki, M. I., Kunzmann, G., Gates, B. C., and Knözinger, H., *J. Phys. Chem.* **91**, 1486 (1987).
28. Basu, P., Panayotov, D., and Yates, J. T., Jr., *J. Amer. Chem. Soc.* **110**, 2074 (1988).
29. Solymosi, F., and Knözinger, H., *J. Chem. Soc. Faraday Trans.* **86**, 389 (1990).